# Efficient Registration of Multiple Range Images for Fully Automatic 3D Modeling

Yulan Guo, Jianwei Wan, Jun Zhang, Ke Xu and Min Lu

*College of Electronic Science and Engineering, National University of Defense Technology, Changsha, China*

Abstract: Multi-view range image registration is a significant and challenging problem for 3D modeling. This paper presents a reference shape based multi-view range image registration algorithm. First, a set of Rotational Projection Statistics (RoPS) features are extracted from the input range images. Next, the reference shape is initialized by selecting a range image from the input. The reference shape is then iteratively updated by registering itself with the remaining range images. The registration between the reference shape and any range image is completed by RoPS feature matching. Finally, all input range images are registered according to their corresponding reference shapes. A number of experiments were performed to test the performance of our algorithm. The experimental results show that the reference shape based algorithm can perform multi-view registration on a mixed set of unordered range images corresponding to several different objects. It is also very accurate and efficient. It outperformed the state-of-the-arts including the spanning tree based and connected graph based algorithms.

## 1 INTRODUCTION

3D models of objects play significant roles in an increasing number of applications including cultural heritage, entertainment, education, medical industry, manufacturing and robotics (Johnson and Bing Kang, 1999; Assfalg et al., 2007; Alexiadis et al., 2013; Guo et al., 2013b). A 3D model can either be created by using Computer Aided Design (CAD) tools or 3D scanning techniques (Chen and Medioni, 1992). Due to the increasing availability of low-cost and dense 3D scanners, range images are becoming more accessible (Guo et al., 2013a; Lei et al., 2013). 3D modeling from range images have became the main research trend when dealing with free-form objects (Dorai et al., 1998). The task of 3D modeling is to register and integrate several range images which are acquired from multiple viewpoints so that the surface of an object can be completely covered (Rusinkiewicz et al., 2002; Mian et al., 2006a).

Multi-view range image registration can be completed either manually or automatically. Since automatic 3D modeling does not require any human intervention (e.g., a calibrated scanner and turntable, or attached markers), it is more applicable to real-world scenarios compared to its manual counterpart (Salvi et al., 2007). The main challenge for automatic

3D modeling is the recovering of the correspondence information between overlapping range image pairs (Mian et al., 2006a). This problem becomes even more difficult when the input range images are unordered and from multiple different objects.

Several multi-view registration algorithms have been proposed to establish correspondences between unordered range images (Huang and Pottmann, 2005). (Huber and Hebert, 2003) registered all pairs of input range images to produce a model graph. The model graph was then used to build a spanning tree which was pose consistent and globally surface consistent. All multi-view range images were finally registered based on the spanning tree. Later, (Masuda, 2009), (Bariya et al., 2012) and (Tombari et al., 2010) also used spanning tree based algorithms to perform multi-view range image registration. However, they employed different features, namely Log-Polar Height Map (LPHM), Signature of Histograms of OrienTations (SHOT) and exponential map, to register any two range images. Given a set of $N_m$ input range images, the computational complexity of the spanning tree based algorithms is $O\left(N_m^2\right)$ as they need to exhaustively register every pair of range images. (Mian et al., 2006a) proposed a connected graph based algorithm, which is more efficient compared to the spanning tree based algorithms. (Guo et al.,

| (a) Object | (b) Local surface | (c) Rotated surface | (d) Projection | (e) Distribution matrix | (f) Statistics | (g) Sub-feature |
|---|---|---|---|---|---|---|
| | $\mathbf{Q'}$ | $\mathbf{Q'}(\theta_k)$ | $\widetilde{\mathbf{Q'}}(\theta_k)$ | $\mathbf{D}$ | $[\,\mu_{mn}, e\,]$ | $f_x(\theta_k)$ |
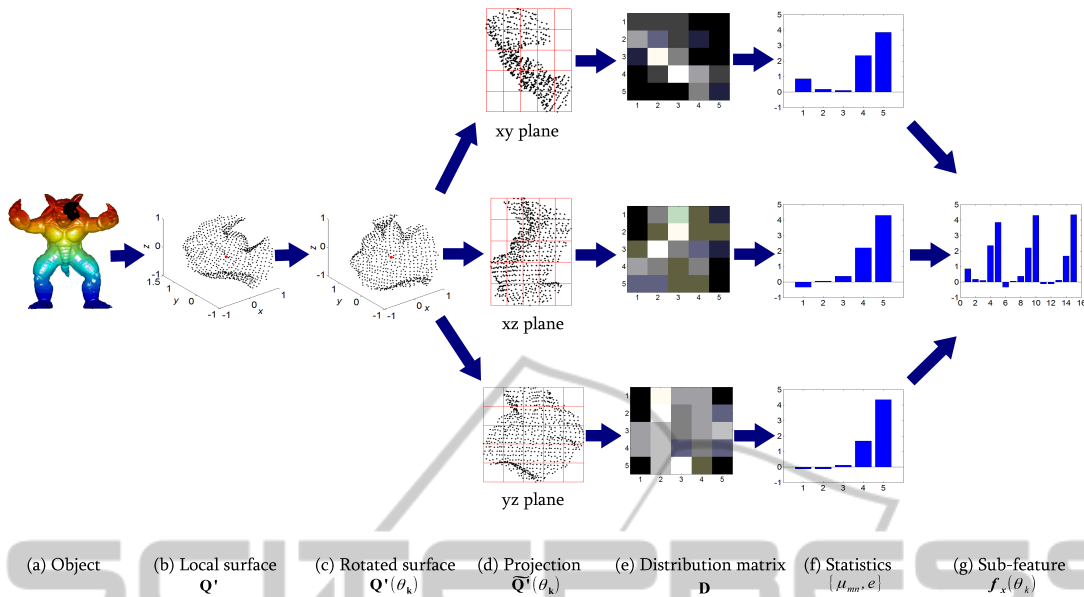
Figure 1: An illustration of the generation of a RoPS feature descriptor for one rotation. Originally shown in (Guo et al., 2013b).

2013c) proposed a Tri-Spin-Image (TriSI) feature for range image representation and also used the connected graph based algorithm for multi-view range image registration. (ter Haar and Veltkamp, 2007) selected quadruples of range images to form incomplete 3D models of an object. These quadruples were further verified and aligned to obtain the final registration result. This algorithm is computational efficient. However, it requires that each quadruple should cover the entire object, and range images which cover a small part of an object cannot be registered (ter Haar and Veltkamp, 2007).

In this paper, we propose a fully automatic, accurate and efficient multi-view range image registration algorithm. The algorithm starts by selecting a range image from all input range images as the initial reference shape. The reference shape is then iteratively updated by performing pairwise registration between itself and the remaining range images in the search space. Consequently, all input range images are registered during the process of reference shape growing. Performance evaluation results show that the proposed reference shape based algorithm is very accurate. It can accomplish multi-view registration on a mixed set of unordered range images corresponding to several different objects. It is also more computationally efficient compared to the state-of-the-arts, including the spanning tree based and connected graph based algorithms.

The rest of this paper is organized as follows. Section 2 presents the local feature extraction and matching techniques. Section 3 describes the reference shape based multi-view range image registration algorithm. Section 4 presents the experimental results of our proposed algorithm, with comparison to the state-of-the-art algorithms.

## 2 FEATURE EXTRACTION AND MATCHING

Local feature extraction and matching forms the basis for the multi-view range image registration algorithm.

### 2.1 Feature Extraction

The local features extracted from range images should be highly discriminative and robust to a set of nuisances including noise and varying mesh resolutions. Based on the range image registration performance achieved by using different local surface features, we select the Rotational Projection Statistics (RoPS) feature for our work as it consistently produces the best results. The superior performance of the RoPS feature for 3D object recognition can also be found in (Guo et al., 2013b). An illustration of the generation of a RoPS feature descriptor is shown in Fig. 1.

Given a range image $I_i$ (in the form of a point cloud), we first convert it into a triangular mesh $\mathcal{M}_i$. We then detect a set of unique and repeatable feature points $\boldsymbol{p}_k^i, k = 1, 2, \ldots, N_i$ from $\mathcal{M}_i$ by performing mesh simplification, resolution control and thresholding (Guo et al., 2013b). For each feature point $\boldsymbol{p}_k^i$

in mesh $\mathcal{M}_i$, a local surface $\mathcal{L}_k^i$ is first cropped from $\mathcal{M}_i$ for a given support radius $r$. Then, a unique and unambiguous Local Reference Frame (LRF) $\mathbf{F}_k^i$ is derived using the eigenvectors of its local surface $\mathcal{L}_k^i$. The points on $\mathcal{L}_k^i$ are aligned with this LRF $\mathbf{F}_k^i$ to make the feature descriptor invariant to rigid transformations (i.e., rotation and translation), resulting in an aligned local surface $\widetilde{\mathcal{L}}_k^i$.

The local surface $\widetilde{\mathcal{L}}_k^i$ is rotated around the $x$, $y$ and $z$ axes respectively by a set of angles. For each rotation, the points on the rotated surface are projected onto three coordinate planes (i.e., the $xy$, $xz$ and $yz$ planes). We first obtain an $L \times L$ distribution matrix $\mathbf{D}$ of the projected points on each plane, and then calculate five statistics (including central moments $\mu_{11}$, $\mu_{21}$, $\mu_{12}$, $\mu_2$ and entropy $e$) for the distribution matrix $\mathbf{D}$. These statistics for all coordinate planes and rotations are concatenated to form an overall RoPS feature $\boldsymbol{f}_k^i$. For more details on the RoPS feature, please refer to (Guo et al., 2013b).

## 2.2 Pairwise Range Image Registration

Given a pair of range images $\mathcal{M}_i$ and $\mathcal{M}_j$, two sets of RoPS features $\boldsymbol{F}^i = \left\{ \boldsymbol{f}_1^i, \boldsymbol{f}_2^i, \ldots, \boldsymbol{f}_{N_i}^i \right\}$ and $\boldsymbol{F}^j = \left\{ \boldsymbol{f}_1^j, \boldsymbol{f}_2^j, \ldots, \boldsymbol{f}_{N_j}^j \right\}$ are respectively extracted from the two range images. For a feature $\boldsymbol{f}_k^i$ in $\mathcal{M}_i$, its corresponding feature $\boldsymbol{f}_k^j$ in $\mathcal{M}_j$ is obtained by searching for the nearest feature in $\boldsymbol{F}^j$. The pair $\left( \boldsymbol{f}_k^i, \boldsymbol{f}_k^j \right)$ are considered a feature correspondence, and their associated points $\boldsymbol{c}_k^{ij} = \left( \boldsymbol{p}_k^i, \boldsymbol{p}_k^j \right)$ are considered a point correspondence. All features in $\boldsymbol{F}^i$ are matched against these features in $\boldsymbol{F}^j$, resulting in a set of point correspondences $\mathcal{C}^{ij} = \left\{ \boldsymbol{c}_1^{ij}, \boldsymbol{c}_2^{ij}, \ldots, \boldsymbol{c}_{N_i}^{ij} \right\}$. For each point correspondence $\boldsymbol{c}_k^{ij}$, a rigid transformation $\mathbf{T}_k^{ij} = \left( \mathbf{R}_k^{ij}, \boldsymbol{t}_k^{ij} \right)$ can be calculated using their point positions $\left( \boldsymbol{p}_k^i, \boldsymbol{p}_k^j \right)$ and LRFs $\left( \mathbf{F}_k^i, \mathbf{F}_k^j \right)$. That is,

$$\mathbf{R}_k^{ij} = \left( \mathbf{F}_k^i \right)^{\mathrm{T}} \mathbf{F}_k^j, \tag{1}$$

$$\boldsymbol{t}_k^{ij} = \boldsymbol{p}_k^i - \boldsymbol{p}_k^j \mathbf{R}_k^{ij}, \tag{2}$$

where $\mathbf{R}_k^{ij}$ is the rotation matrix and $\boldsymbol{t}_k^{ij}$ is the translation vector of the rigid transformation $\mathbf{T}_k^{ij}$.

A set of $N_i$ plausible transformations are calculated from the point correspondences $\mathcal{C}^{ij}$. These transformations are further grouped and verified to produce a robust transformation $\mathbb{T}^{ij}$. The two range images $\mathcal{M}_i$ and $\mathcal{M}_j$ are then coarsely registered using
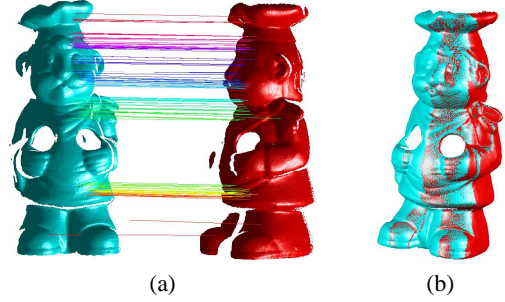


Figure 2: An illustration of pairwise range image registration. (a) A pair of range images with the correct point correspondences. (b) Registered range images. (Figure best seen in color.)

the transformation $\mathbb{T}^{ij}$. The registration is further refined using an improved Iterative Closest Point (ICP) algorithm by repeatedly generating pairs of closest points in the two range images and minimizing the residual error (Besl and McKay, 1992). Note that, a recently proposed spare ICP algorithm (Bouaziz et al., 2013) can alternatively be used to deal with challenging datasets affected by noise and outliers. An illustration of pairwise range image registration is shown in Fig. 2. Fig. 2(a) shows a pair of range images with the correct point correspondences, Fig. 2(b) shows the two registered range images.

# 3 MULTI-VIEW RANGE IMAGE REGISTRATION

So far we have introduced a RoPS feature matching based algorithm for pairwise range image registration. In this section, we propose a reference shape based algorithm for multi-view range image registration. Fig. 3 shows an illustration of the proposed multi-view range image registration algorithm. Moreover, the whole process is given in Algorithm 1.

Given a set of meshes $\left\{ \mathcal{M}_1, \mathcal{M}_2, \ldots, \mathcal{M}_{N_m} \right\}$, we initialize the search space $\boldsymbol{\Phi}$ with all the input meshes. The algorithm then starts by selecting a mesh from the search space as the initial reference shape $\mathcal{R}_1$, which iteratively grows by performing pairwise registration between itself and the remaining meshes in the search space.

For a mesh $\mathcal{M}_i$ in the search space, we use the RoPS matching based pairwise registration algorithm to register it to the reference shape $\mathcal{R}_1$. If the number of overlapping points is more than $\tau_o$ times of the number of vertices in $\mathcal{M}_i$, we consider that $\mathcal{M}_i$ is successfully registered to $\mathcal{R}_1$. We then add the vertices in $\mathcal{M}_i$, whose shortest distances to $\mathcal{R}_1$ are more than the average mesh resolution, to the reference shape

**(a) Input Meshes**          **(b) Reference Shape Growing**          **(c) Multi-view Registration**          **(d) 3D Models**
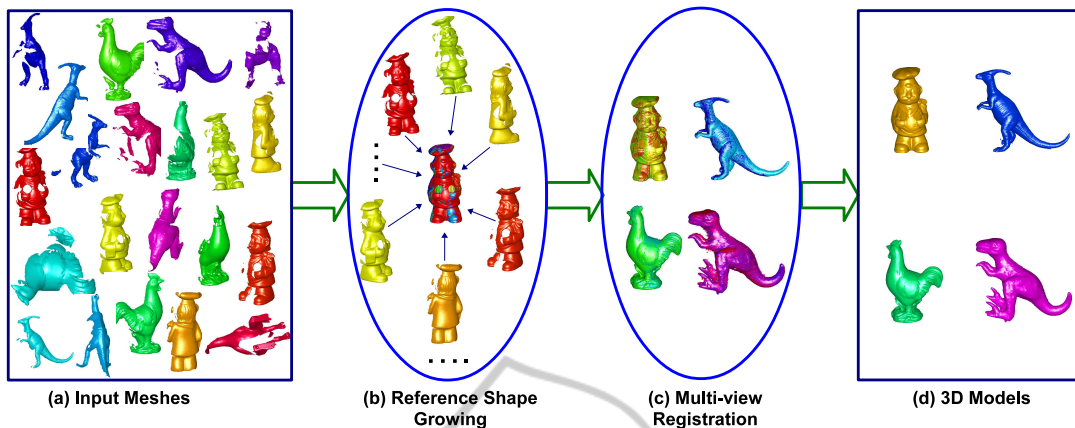
Figure 3: An illustration of the proposed multi-view range image registration algorithm.

$\mathcal{R}_1$. Consequently, the reference shape $\mathcal{R}_1$ is updated. We then need to generate RoPS features for the newly updated reference shape. Since the RoPS features have already been extracted in the previous reference shape and the mesh $\mathcal{M}_i$. We therefore, generate RoPS features for the updated reference shape by looking for its closest feature points in the previous reference shape and $\mathcal{M}_i$. Note that, this approach greatly improves the computational efficiency of feature extraction as it does not require any feature calculation during the process of reference shape growing.

Once the mesh $\mathcal{M}_i$ is checked, it is then removed from the search space $\boldsymbol{\Phi}$, and the transformation information between $\mathcal{M}_i$ and the reference shape $\mathcal{R}_1$ is stored. The next mesh $\mathcal{M}_{i+1}$ in the search space $\boldsymbol{\Phi}$ is selected by turn to be registered to the updated reference shape. The growing process of the reference shape continues until either all the meshes have been registered to $\mathcal{R}_1$, or none mesh in the search space $\boldsymbol{\Phi}$ can further be registered to $\mathcal{R}_1$. Note that, during the process of iterations, the surface (i.e., points) of $\mathcal{R}_1$ gradually grows into a whole complete 3D shape. Meanwhile, the pose of $\mathcal{R}_1$ keeps unchanged. Once the growing process for the reference shape $\mathcal{R}_1$ stops, the rigid transformations between all these registered meshes and $\mathcal{R}_1$ are already known. We then transform these meshes to the coordinate frame of $\mathcal{R}_1$. Consequently, these meshes are coarsely registered.

In order to cope with the cases where the meshes may correspond to several different objects, the algorithm continues to initialize a new reference shape $\mathcal{R}_2$ by picking up a mesh from the remaining meshes in the search space. The reference shape $\mathcal{R}_2$ grows using the same technique as for $\mathcal{R}_1$. Consequently, all the meshes corresponding to reference shape $\mathcal{R}_2$ are coarsely registered. This process continues until none initial reference shape can be built any more. Finally, all these input meshes can separately be registered to

their corresponding reference shapes.

Once the meshes corresponding to a specific reference shape are coarsely registered, these registrations are further refined with a multi-view fine registration algorithm (e.g., (Williams and Bennamoun, 2001)). The multi-view fine registration algorithm minimizes the overall registration error of multiple meshes, and distributes any registration errors evenly over the complete 3D model. Finally, a continuous and seamless 3D model is reconstructed for each reference shape by using an integration and surface reconstruction algorithm (Curless and Levoy, 1996).

Note that, the proposed algorithm is fully automatic and can be performed without any manual intervention. It does not require any prior information about the sensor position, the shapes of objects, viewing angles, overlapping pairs, order of meshes, or number of objects. In our case, a user can treat the modeling process as a "black box". The only thing one needs to do is to import all scanned range images to the system, and to collect the complete 3D models after a while of running.

Compared to the spanning tree based algorithms (Huber and Hebert, 2003; Bariya et al., 2012; Tombari et al., 2010; Masuda, 2009), the advantages of the proposed reference shape based algorithm are obvious. First, it performs multi-view range image registration more efficiently, as demonstrated in Section 4.3. For a set of $N_m$ range images, its computational complexity is $O\left(N_m\right)$ compared to $O\left(N_m^2\right)$ for the spanning tree based algorithms. Second, it is capable to perform registration of multiple range images corresponding to several different objects, rather than from only a single object, as further demonstrated in Section 4.4. Third, it does not suffer from cumulative registration errors because all meshes of an object are registered to the same reference shape. In contrast, the registration errors between any two meshes may

**Algorithm 1:** Reference shape based multi-view registration.

1: **Input**: Meshes $\{\mathcal{M}_1, \mathcal{M}_2, \ldots, \mathcal{M}_{N_m}\}$.
2: **Initialization**: Search space $\Phi \leftarrow \{\mathcal{M}_1, \mathcal{M}_2, \ldots, \mathcal{M}_{N_m}\}$. Number of reference shape $n_s \leftarrow 0$.
3: **while** $\Phi$ is not empty **do**
4:     $n_s \leftarrow n_s + 1$.
5:     Initialize reference shape $\mathcal{R}_{n_s}$ with a mesh from $\Phi$.
6:     **repeat**
7:       Select a mesh $\mathcal{M}_i$ from $\Phi$ and register it to $\mathcal{R}_{n_s}$.
8:       **if** Successfully registered **then**
9:         Update the reference shape $\mathcal{R}_{n_s}$ by adding new points from $\mathcal{M}_i$.
10:        Extract RoPS features for the updated $\mathcal{R}_{n_s}$.
11:        Store the transformation between $\mathcal{R}_{n_s}$ and $\mathcal{M}_i$.
12:       **end if**
13:       Remove the mesh $\mathcal{M}_i$ from $\Phi$.
14:     **until** No mesh in $\Phi$ can be successfully registered to $\mathcal{R}_{n_s}$
15: **end while**
16: **Output**: Reference shapes $\{\mathcal{R}_1, \mathcal{R}_2, \ldots, \mathcal{R}_{n_s}\}$, and the transformations between reference shapes and their corresponding meshes.

accumulate through the path in a spanning tree based algorithm.

# 4 EXPERIMENTAL RESULTS

In this section, we present the performance of our algorithm when tested in different circumstances. We also compare our algorithm to the state-of-the-arts.

## 4.1 Experimental Setup

We used the UWA 3D Modeling Dataset (Mian et al., 2006a) to conduct experiments. The dataset consists of 22, 16, 16, and 21 range images respectively for four objects, namely the Chef, Chicken, Parasaurolophus and T-Rex. These range images were acquired with a Minolta Vivid 910 scanner. We manually aligned any two range images $\mathcal{M}_i$ and $\mathcal{M}_j$ and further refined the alignment using the ICP algorithm to calculate the ground truth rotation $\mathbf{R}_{GT}^{ij}$ and translation $t_{GT}^{ij}$ between them. We then measured the degree of overlap as the ratio of overlapping points to the average number of points of the two aligned range images.

For a given pair of range images $\mathcal{M}_i$ and $\mathcal{M}_j$, the accuracy of registration is measured by two errors: the rotation error $\varepsilon_r^{ij}$ and translation error $\varepsilon_t^{ij}$. The formulas for calculating the rotation error $\varepsilon_r^{ij}$ between the estimated rotation $\mathbf{R}_E^{ij}$ and the ground truth rotation $\mathbf{R}_{GT}^{ij}$, and the translation error $\varepsilon_t^{ij}$ between the estimated translation $t_E^{ij}$ and the ground truth translation $t_{GT}^{ij}$, is given in (Mian et al., 2006b). A registration of two range images was reported as correct if the rotation error was less than $5°$ and the translation error was less than $5d_{res}$, where $d_{res}$ stands for average mesh resolution. Otherwise, it was considered as an incorrect registration.

## 4.2 Multi-view Registration of a Single Object

We performed multi-view registration independently on range images of each individual object. Fig. 4 illustrates the range images and the multi-view coarse registration results of the Chicken and Parasaurolophus. Although these range images were scanned from different viewpoints and organized without any order, they were accurately registered. No visually noticeable defects or seams can be found in the registered range images, even in the featureless parts of the objects (e.g., the tail of the Parasaurolophus in Fig. 4(d)).

In order to quantitatively analyze the accuracy of our multi-view registration algorithm, we present the number of correctly registered range images, and the average registration errors of each individual object in Table 1. It can be seen that all input range images of the four individual objects were correctly registered. The average rotation and translation errors of the four objects were less than $2.5°$ and $2d_{res}$, respectively. Note that these results were achieved by using only the multi-view coarse registration algorithm. These yet accurate results can further be improved by the subsequent fine registration algorithm (e.g., the multi-view ICP). Generally, our algorithm enables multi-view coarse registration to be performed automatically and accurately.

## 4.3 Robustness to the Number of Input Meshes

In order to evaluate the computational efficiency of the multi-view registration algorithm with respect to the number of input meshes, we progressively selected a subset of the range images to perform multi-view registration. For each fixed number of input
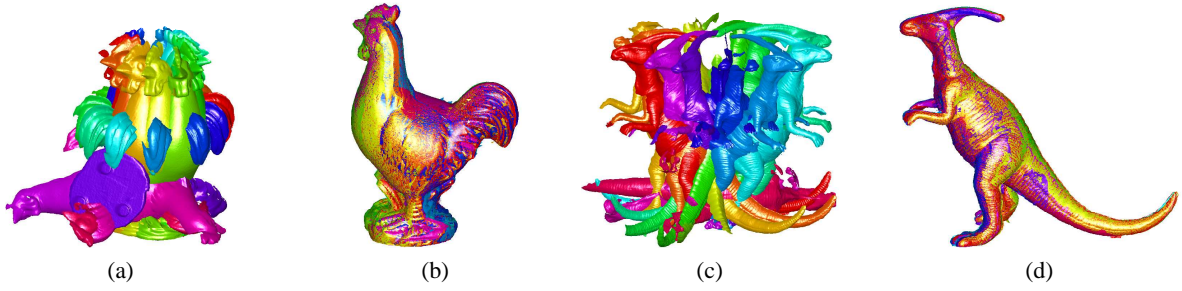
Figure 4: An illustration of multi-view coarse registration results. (a) Range images of the Chicken. (b) Multi-view registration result of the Chicken. (c) Range images of the Parasaurolophus. (d) Multi-view registration result of the Parasaurolophus (Figure best seen in color).

Table 1: Multi-view coarse registration results on range images of four individual objects.

|  | Chef | Chicken | Parasaurolophus | T-Rex |
|---|---|---|---|---|
| #range images | 22 | 16 | 16 | 21 |
| #registered range images | 22 | 16 | 16 | 21 |
| Rotation error $\varepsilon_r$ (°) | 2.2117 | 1.0075 | 1.0634 | 1.3722 |
| Translation error $\varepsilon_t$ ($d_{res}$) | 1.6460 | 1.0936 | 1.6634 | 1.9165 |



(a) Chef          (b) Chicken          (c) Parasaurolophus          (d) T-Rex
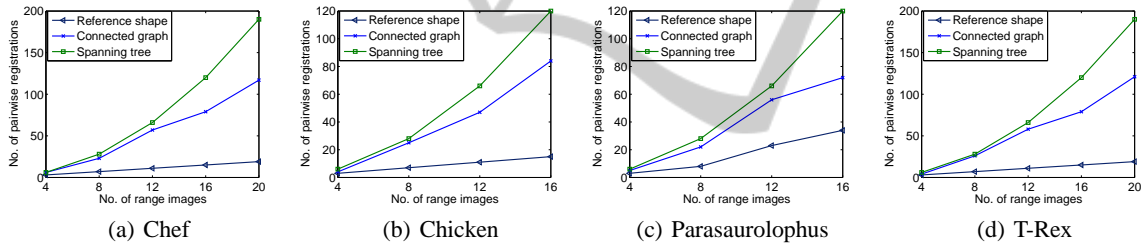
Figure 5: Robustness with respect to the number of input meshes.



(a) Input meshes          (b) Chef          (c) Chicken          (d) Parasaurolophus          (e) T-Rex
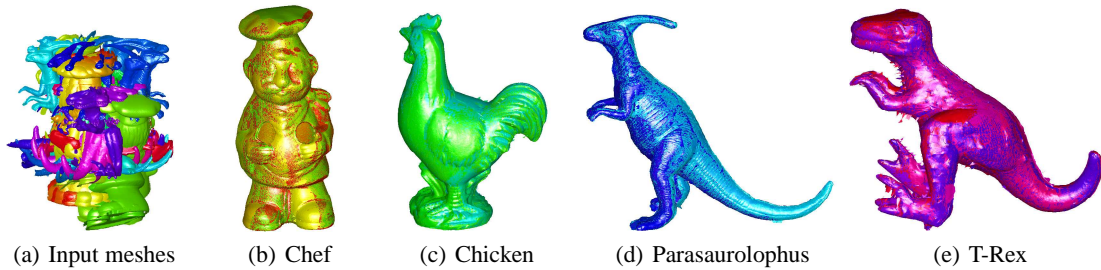
Figure 6: Multi-view coarse registration of range images corresponding to multiple objects(Figure best seen in color).

Table 2: Multi-view coarse registration results on mixed range images of the four objects.

|  | Chef | Chicken | Parasaurolophus | T-Rex |
|---|---|---|---|---|
| #range images | 22 | 16 | 16 | 21 |
| #registered range images | 22 | 16 | 16 | 21 |
| Rotation error $\varepsilon_r$ (°) | 1.8656 | 1.1674 | 0.4029 | 1.3789 |
| Translation error $\varepsilon_t$ ($d_{res}$) | 1.3627 | 1.0976 | 0.9914 | 1.9128 |
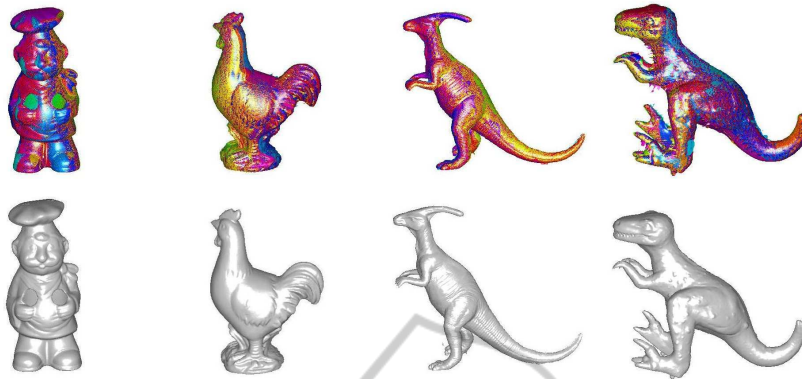
Figure 7: 3D modeling results (Figure best seen in color.)

meshes, we counted the number of pairwise registrations which were needed to complete the multi-view registration. The results for each of the four objects are shown in Fig. 5. We also present the results of the state-of-the-arts including the spanning-tree based algorithms (Huber and Hebert, 2003; Masuda, 2009), and the connected graph based algorithm (Mian et al., 2006a). The spanning tree based algorithms required $C_2^{N_m}$ pairwise registrations to perform a multi-view registration, where $N_m$ is the number of input range images and $C$ stands for combinations. Therefore, their computational complexity is $O\left(N_m^2\right)$. Our reference shape based algorithm showed a significant improvement compared to both the spanning tree based and the connected graph based algorithms. It usually completed the multi-view registration of $N_m$ range images with only $N_m - 1$ pairwise registrations. Taking the 20 input range images of the Chef as an example (see Fig. 5(a)), the numbers of pairwise registrations for the spanning tree based, connected graph based and reference shape based algorithms were 190, 117 and 19, respectively. The improvement factor of our reference shape based algorithm over the spanning tree based algorithm was $\frac{190}{19} = 10$. Moreover, the advantage in efficiency of the reference shape based algorithm becomes even more significant as the number of input range images increases.

## 4.4 Multi-view Registration of Multiple Objects

In order to further demonstrate the capability of our algorithm to simultaneously register multiple mixed range images corresponding to multiple objects, we used all the range images of the four objects as an input. These range images were mixed and were registered using our reference shape based algorithm. As results, four reference shapes were produced by

our algorithm. The totally 75 input range images are shown in Fig. 6(a), and the coarse registration results for the four reference shapes are respectively shown in Fig. 6(b-e). It can be seen that, all these input range images were separately registered according to their corresponding reference shapes. Moreover, although fine registration was not applied to these registration results, no visually noticeable seams can be found in any of the registered range images.

We also present the quantitative results in Table 2. These results were almost the same as these reported in Table 1. This observation clearly indicates that the range image registration accuracy of an object could not be affected by the existence of range images corresponding to other objects. That is, our algorithm is able to perform multi-view registration correctly from a mixed and unordered range images which correspond to several different objects.

## 4.5 3D Modeling Results

In order to test the whole pipeline for 3D object modeling, we used the range images of the Chef, Chicken, Parasaurolophus and T-Rex as inputs. We extracted RoPS features from each range image, and performed multi-view range image registration using the reference shape based algorithm. We then integrated the range images corresponding to each reference shape, producing a reconstructed complete 3D model. The multi-view registration results and reconstructed 3D models of these objects are shown in Fig. 7. These results clearly demonstrate that our algorithm is capable of reconstructing 3D models by seamlessly merging multiple range images.

## 5 CONCLUSIONS

In this paper, we presented a reference shape based algorithm for multi-view range image registration. We tested the performance of our algorithm on multiple range images from either one object or multiple objects. Experimental results show that the proposed algorithm can perform multi-view range image registration on mixed and unordered range images which correspond to different objects. We also tested the robustness of our algorithm with respect to varying numbers of input range images. It is shown that the proposed algorithm is more computationally efficient compared to the state-of-the-art methods. We further demonstrated the effectiveness of the proposed algorithm by performing 3D modeling. Overall, the proposed algorithm is accurate, efficient and robust.

## REFERENCES

Alexiadis, D., Zarpalas, D., and Daras, P. (2013). Real-time, full 3-D reconstruction of moving foreground objects from multiple consumer depth cameras. *IEEE Transactions on Multimedia*, 15(2):339–358.

Assfalg, J., Bertini, M., Bimbo, A., and Pala, P. (2007). Content-based retrieval of 3-D objects using spin image signatures. *IEEE Transactions on Multimedia*, 9(3):589–599.

Bariya, P., Novatnack, J., Schwartz, G., and Nishino, K. (2012). 3D geometric scale variability in range images: Features and descriptors. *International Journal of Computer Vision*, 99(2):232–255.

Besl, P. and McKay, N. (1992). A method for registration of 3-D shapes. *IEEE Transactions on Pattern Analysis and Machine Intelligence*, 14(2):239–256.

Bouaziz, S., Tagliasacchi, A., and Pauly, M. (2013). Sparse iterative closest point. *Computer Graphics Forum (Special Issue of Symposium on Geometry Processing)*, 32(5):1–11.

Chen, Y. and Medioni, G. (1992). Object modelling by registration of multiple range images. *Image and vision computing*, 10(3):145–155.

Curless, B. and Levoy, M. (1996). A volumetric method for building complex models from range images. In *23rd Annual Conference on Computer Graphics and Interactive Techniques*, pages 303–312.

Dorai, C., Wang, G., Jain, A. K., and Mercer, C. (1998). Registration and integration of multiple object views for 3D model construction. *IEEE Transactions on Pattern Analysis and Machine Intelligence*, 20(1):83–89.

Guo, Y., Bennamoun, M., Sohel, F., Wan, J., and Lu, M. (2013a). 3D free form object recognition using rotational projection statistics. In *IEEE 14th Workshop on the Applications of Computer Vision*, pages 1–8.

Guo, Y., Sohel, F., Bennamoun, M., Lu, M., and Wan, J. (2013b). Rotational projection statistics for 3D local

surface description and object recognition. *International Journal of Computer Vision*, 105(1):63–86.

Guo, Y., Sohel, F., Bennamoun, M., Lu, M., and Wan, J. (2013c). TriSI: A distinctive local surface descriptor for 3D modeling and object recognition. In *8th International Conference on Computer Graphics Theory and Applications*, pages 86–93.

Huang, Q. and Pottmann, H. (2005). Automatic and robust multi-view registration. Technical report, Tsinghua University.

Huber, D. and Hebert, M. (2003). Fully automatic registration of multiple 3D data sets. *Image and Vision Computing*, 21(7):637–650.

Johnson, A. E. and Bing Kang, S. (1999). Registration and integration of textured 3D data. *Image and Vision Computing*, 17(2):135–147.

Lei, Y., Bennamoun, M., Hayat, M., and Guo, Y. (2013). An efficient 3D face recognition approach using local geometrical signatures. *Pattern Recognition*.

Masuda, T. (2009). Log-polar height maps for multiple range image registration. *Computer Vision and Image Understanding*, 113(11):1158–1169.

Mian, A., Bennamoun, M., and Owens, R. (2006a). Three-dimensional model-based object recognition and segmentation in cluttered scenes. *IEEE Transactions on Pattern Analysis and Machine Intelligence*, 28(10):1584–1601.

Mian, A., Bennamoun, M., and Owens, R. A. (2006b). A novel representation and feature matching algorithm for automatic pairwise registration of range images. *International Journal of Computer Vision*, 66(1):19–40.

Rusinkiewicz, S., Hall-Holt, O., and Levoy, M. (2002). Real-time 3D model acquisition. In *ACM Transactions on Graphics*, volume 21, pages 438–446. ACM.

Salvi, J., Matabosch, C., Fofi, D., and Forest, J. (2007). A review of recent range image registration methods with accuracy evaluation. *Image and Vision Computing*, 25(5):578–596.

ter Haar, F. B. and Veltkamp, R. C. (2007). Automatic multiview quadruple alignment of unordered range scans. In *IEEE International Conference on Shape Modeling and Applications*, pages 137–146.

Tombari, F., Salti, S., and Di Stefano, L. (2010). Unique signatures of histograms for local surface description. In *European Conference on Computer Vision*, pages 356–369.

Williams, J. and Bennamoun, M. (2001). Simultaneous registration of multiple corresponding point sets. *Computer Vision and Image Understanding*, 81(1):117–142.